Author/s:
Karami, S;TALEI, M;Hawkes, ER

Title:
Local extinction and reignition in a turbulent lifted flame

Date:
2015

Citation:
Karami, S., TALEI, M. & Hawkes, E. R. (2015). Local extinction and reignition in a turbulent lifted flame. Yang, Y (Ed.) Smith, N (Ed.) Proceedings of the Australian Combustion Symposium, pp.168-171. The Combustion Institute Australia & New Zealand Section.

Persistent Link:
https://hdl.handle.net/11343/258644

Proceedings of the Australian Combustion Symposium
December 7-9, 2015, The University of Melbourne

Local extinction and reignition in a turbulent lifted flame

Shahram Karami[1,*], Mohsen Talei[2], Evatt R. Hawkes[1,3]
[1] School of Photovoltaic and Renewable Energy
The University of New South Wales, NSW 2052, Australia
[2] Department of Mechanical Engineering
University of Melbourne, Melbourne, VIC 3010, Australia
[3] School of Mechanical Engineering
The University of New South Wales, NSW 2052, Australia

Abstract

Direct numerical simulation (DNS) was used to analyse local extinction and reignition in a lifted turbulent flame. The edge flame propagation velocity appears to be dependent on the scalar dissipation rate consistent with previous experimental and numerical studies. This dependency is analysed with a model proposed for laminar triple flames, showing a good agreement for moderate scalar dissipation rates and an under- and over-predictions of the DNS results in very low and high scalar dissipation rates, respectively. These discrepancies are then explained based on the model's assumptions. The extinction and reignition are also analysed separately where the distinction is made based on the average hole diameter. It is revealed that during the extinction process, the edge flame is primarily a nonpremixed flame and propagation velocity reduces in a non-linear manner as scalar dissipation rate increases. In the reignition process, the flame experiences a wide range of premixed and non-premixed modes and the edge propagation velocity, conditionally averaged on the scalar dissipation rate decreases linearly when the scalar dissipation rate increases.

Keywords: Local extinction, Reignition, Strain rate, Curvature.

1. Introduction

The rate of mixing between fuel and air plays an important role in the flame stability and pollutant emissions for nonpremixed flames. A low mixing rate will affect the device efficiency and produce pollution, whereas the mixing rate higher than a specific value will result in local or even global extinction. As a result, local extinction and reignition have received a great attention in the literature.

Extinction and reignition have been a topic of a number of numerical studies. For instance, the extinction of a laminar triple flame with a pair of vortices was studied by Favier and Vervisch [1, 2] wherein it was shown that the scalar dissipation rate is the controlling parameter. However, it was observed that the scalar dissipation of growing holes is lower than that which has initiated the local extinction. In another study of a non-premixed flame in a counter-flow configuration under oscillating strain-rate conditions [3], it was observed that the flame was extinguished as the strain rates exceed the critical extinction strain rate of steady flames. In a DNS study of a piloted flame, Pantano [4] observed that extinction is controlled by the scalar dissipation rate. Furthermore, some of the extinction events were encountered in regions with a higher scalar dissipation rate than that for the extinction limit in a laminar flame. Sripakagorn et. al. [5] studied the effect of turbulence on extinction and reignition of flame holes in a isotropic three-dimensional decaying turbulence with a single-step chemistry model and an assumption of negligible density variations. They found that the edge-flame propagation and engulfment of neighbour hot products to the unburned portion of stoichiometric surface are the main mechanisms of reignition. In addition, independent flamelet scenario has a minor contribution in reignition. Pantano and Pullin [6] proposed a model for local extinction holes where the holes dynamics are assumed to be controlled by the edge-propagation velocity which is only a function of the scalar dissipation rate in their theory. A general transport equation for the joint probability density function of the hole area and scalar dissipation rate was proposed. A simplified form of this equation was solved for small holes. They assumed that the net rate of production–distribution of the holes area and the folding effects of mixture fraction iso-surfaces are negligible.

The physical mechanisms of extinction and reignition in turbulent lifted flames are not yet understood. Experimental studies reveal that large vortical structures and high strain rates on the stoichiometric surface can extinguish the flame [7, 8]. Some recent experimental studies with access to high-resolution measurements discuss the effects of the scalar dissipation rate; however, these studies are limited to two-dimensional measurements. One should note that interpreting the observations of two-dimensional measurements in turbulent lifted flames for which the third dimension is crucially important [9] can be misleading. The authors are not aware of any numerical studies of extinction and reignition in turbulent lifted flames. The available studies are limited to simpler configurations and hence their findings cannot be easily extended to turbulent lifted flames.

Therefore, the main focus of this paper is to analyse extinction and reignition in a lifted turbulent flame using direct numerical simulation (DNS). The analysis will reveal the mechanisms involved in

* Corresponding author:
Phone: (+61) 2 9385 4602
Email: s.karami@unsw.edu.au

extinction and reignition and the role of key parameters, namely the scalar dissipation rate and normalised flame index.

2. Description of the DNS database

2.1 Configuration

The DNS data used here was previously introduced in our previous study on the stabilisation mechanism of a turbulent lifted flame [10]. The details of the run are given in Ref. [10], so only a brief overview is given here. The configuration is a slot-jet flame where fuel is injected at the velocity, U_j, into a slower co-flow of oxidiser having the velocity $0.01U_j$. The mean inlet axial velocity, U_{in}, was specified to vary between the pure streams using a *tanh* profile with the momentum thickness of 0.05H, where H is the jet width. Turbulence in the fuel jet was specified with a frozen turbulent velocity field, based on a prescribed turbulent Passot-Pouquet energy spectrum, which is convected into the domain by applying Taylor’s hypothesis. A uniform grid spacing of 0.02H was used in the streamwise and spanwise directions, which is approximately twice the Kolmogorov length scale, considered to be a good resolution in DNS [11]. An algebraically stretched mesh was used in the transverse direction which maintained uniform spacing of 0.02H in $|y| < 5H$, where y is the transverse coordinate, and less than 3 % stretching in the region of $|y| > 5H$. The simulation was performed for 18.0 jet flow through times, $t_j = L_x/U_j$, where L_x is the streamwise domain length.

Table 1: Numerical and physical parameters of the simulation.

Description	**Value**
Domain size ($L_x \times L_y \times L_z$)	16H×24H×6H
Number of grid points ($N_x \times N_y \times N_z$)	800×800×300
Mean inlet jet Mach number (U_j/a_{ref})	0.48
Laminar co-flow Mach number (U_{co}/a_{ref})	0.001
Jet non-dimensional temperature (T_{jet})	2.5
Co-flow non-dimensional temperature ($T_{co\text{-}flow}$)	2.5
Jet Reynolds number (Re)	5280
Inlet velocity fluctuation intensity	5%
Fuel mass fraction in the fuel stream ($Y_{F,o}$)	1.0
Oxidiser mass fraction in the oxidiser stream ($Y_{O,o}$)	0.233
Stoichiometric oxidiser to fuel mass ratio (r)	4.0
Heat-release parameter (α)	0.86
Zel’dovich number (β)	5.0
Non-dimensionalisation Damköhler number (Da)	800
Lewis number (Le)	1.0
Prandtl number (Pr)	0.7

2.2 Physical model and parameters

To limit the computational cost, a single-step irreversible reaction of $F+rO \rightarrow (1+r)P$ with an Arrhenius source term was used. A modified activation energy approach, initially developed by Garrido-López and Sarkar [12], was used to capture the realistic dependence of laminar burning velocity on equivalence ratio that is typical of the hydrocarbon fuels. A comprehensive justification of the choice of chemistry model is described in our previous article [10]. The reaction and thermochemical parameters are chosen to result in the H/δ_L and U_j/S_L being comparable to experimentally measured methane flames[13], where δ_L is the laminar flame thickness and S_L is the laminar burning velocity.

The parallel DNS code, S3D_SC was employed. S3D_SC is a one-step chemistry version of S3D, developed at Sandia National Laboratories [14]. The compressible Navier-Stokes, sensible energy, and species transport equations are solved on a structured 3D Cartesian mesh using high order methods [14]. Non-reflecting outflow boundary conditions are used in the streamwise and transverse directions, and periodic boundary conditions are applied in the spanwise direction [15-17]. Other simulation parameters are summarised in Table 1.

3. Mathematical background

In this study focussing on extinction and reignition, it is useful to define a concept of flame edges, which separate the burning and nonburning regions of a mixture-fraction isosurface. Following previous studies [4, 10, 18, 19] the flame edges are defined as the intersection points of a mixture-fraction iso-surface with a product mass-fraction iso-surface. The mixture-fraction iso-value is 0.07, which corresponds to the mixture-fraction having the highest flame speed in a one-dimensional flat premixed laminar flame, while the product iso-value was selected as the value corresponding to the maximum reaction rate in the same flame. A sensitivity analysis of the edge-flame statistics to these criteria is shown in Ref. [10].

The holes identified using this methodology were extensively visualised to understand the holes behaviour and their interaction with each other. The extinction holes might grow and shrink independently, split into multiple holes, and/or merge with neighbour holes, which is consistent with the observations in previous experimental studies [7, 20-22].

As an orientation, first we discuss the behaviour of all extinction holes away from the flame base. Then, we focus on extinction and reignition of individual holes. For this purpose, *thirty* individual holes with no splitting and merging and far from other neighbouring holes were selected to minimise the hole-hole interaction. These individual holes, however, do not have a simple structure and are commonly convoluted due to the effects of turbulence. This is in contrast to the assumption made by Pantano and Pullin [6] in their model for local extinction holes.

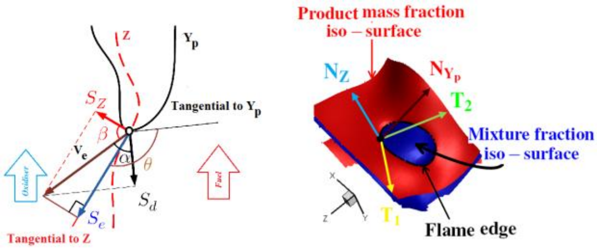

Figure 1. Schematic of the hole and edge propagation velocities.

The edge-flame displacement speed, S_e, is defined as the motion of the flame edge relative to the flow (defined positive if towards reactants), projected into the plane of the mixture-fraction iso-surface. The edge speed is given in terms of the product mass-fraction self-displacement speed S_d, the mixture-fraction self-displacement speed S_z, and the inner product of the normal vectors to product and mixture-fraction iso-surfaces k as [19]:

$$S_e^* = \frac{S_d^* - kS_Z^*}{\sqrt{1-k^2}}, \rho_u S_d^* = \frac{\rho DY_P/Dt}{|\nabla Y_P|} \text{ and } \rho_u S_Z^* = \frac{\rho DZ/Dt}{|\nabla Z|}. \quad (1)$$

The normalised flame index (NFI) [23] is also used here to distinguish between premixed and nonpremixed combustion modes and is defined as:

$$\mathrm{NFI} = \frac{\mathbf{N_Z}.\mathbf{N_{Yp}}}{|\mathbf{N_Z}.\mathbf{N_{Yp}}|}. \quad (2)$$

4. Results and discussion

For orientation, the dependence of the edge-flame propagation velocity on scalar dissipation rate is compared with the proposed model by Pantano and Pullin [6]. In those studies the edge-flame propagation velocity was parameterised as a function of

$$\varepsilon = \frac{l_{LF}}{L/\beta}, \quad (3)$$

where l_{LF} and L are respectively the laminar flame and mixing layer thicknesses and defined as,

$$l_{LF} = \frac{\lambda}{\rho C_P S_L} \text{ and } L/\beta = \sqrt{\frac{2\lambda}{\rho C_P \chi}}, \quad (4)$$

where β is the Zel'dovich number, ρ is the density, C_P is the specific heat coefficient, λ is the thermal conductivity and χ is the scalar dissipation rate. Pantano and Pullin [6] assumed that for small holes, i.e. holes which can be characterised by their area, the edge-flame propagation velocity can be modelled as:

$$\frac{S_e^*}{S_L} = 1 - \frac{1+\frac{1}{\frac{\varepsilon}{\varepsilon_{ex}}-1}}{1+\frac{1}{\frac{\varepsilon_0}{\varepsilon_{ex}}-1}}, \quad (5)$$

where ε_{ex} is the value of extinction limit beyond which no flame exists and ε_0 is the value of ε where S_e^* is zero [6]. The joint PDF of the edge-flame propagation velocity and ε for all holes in the region of 5<x<12 is presented in Fig 2. The black circles are the conditional average of edge-flame propagation velocity on ε and the red circles are the model presented by equation 5. There is a reasonable agreement between the model and the DNS results in particular for moderate scalar dissipation rates. The departure of the conditional mean from the model for low ε values can be due to the interaction of holes boundaries in the healing process. When the extinction holes heal, edge flames seek to meet and close the holes completely. The visualisation of the healing process shows that when the holes reach to a diameter less than two times of the thermal flame thickness, the healing accelerates because of the edge-flames interactions. There is also a deviation from the model for high ε values and the model over-predicts the edge-flame propagation velocity. The main reason for this difference is that the model was developed for small and less disturbed holes; however, the holes in this study are highly contorted and are as big as three times of the jet width.

Now, the question arises, how the scalar dissipation rate contributes to the extinction and reignition processes and what mode of combustion, e.g. premixed or non-premixed is dominant? To answer these questions, extinction and reignition of thirty holes are analysed where the distinction of reignition from extinction was achieved using the rate of change in the average hole radius. The average radius of each hole at each instant was calculated by averaging the distance of the edge-flame locations from centroid of the hole.

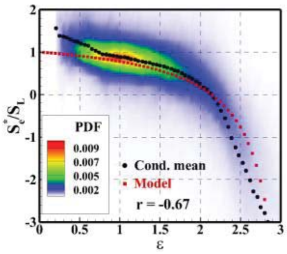

Figure 2. The joint PDF of edge-flame propagation velocity and ε (black circles are conditional means and the red squares are the model proposed by Pantano and Pullin [6]).

4.1 Extinction mechanism

The joint PDF of the edge propagation velocity and the scalar dissipation rate during extinction is shown in Fig. 3a. The edge propagation velocity is negatively correlated with the scalar dissipation rate. The joint PDF is narrow with low fluctuations over the conditional mean. The conditional mean shows a non-linear behaviour as expected for extinction events [24]. The joint PDF of the edge-propagation velocity and scalar dissipation rate also shows that even though a high scalar dissipation rate is required for formation of the holes, the hole can grow with lower values of scalar dissipation rate [2].

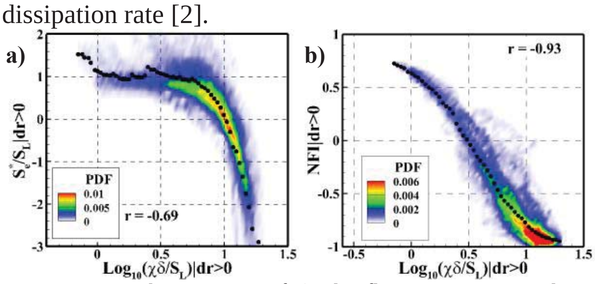

Figure 3. The joint PDF of a) edge-flame propagation velocity and b) NFI when the local extinction occurs with the normalised scalar dissipation rate (black circles are conditional means).

The normalised flame index (NFI) which is widely used to distinguish premixed from non-premixed flames is presented in Fig. 3b. The joint PDF of the NFI and scalar dissipation rate shows the dominant presence of non-premixed flames in the local extinction process. These observations suggest that local extinctions occur when a highly straining turbulent structure intrudes into the flame sheet, resulting in squeezing of the product mass fraction and mixture-fraction iso-surfaces such that the flame could not be sustained due to the excessive dissipation of heat.

4.2 Reignition mechanism

In contrast to the extinction process, the conditional edge-flame propagation velocity on the scalar dissipation rate exhibits a mostly linear (but still decreasing) response to an increase in the scalar dissipation rate from low to moderate values as can be observed in Fig. 4a. The edge-propagation velocity at low values of scalar dissipation rate corresponding to the final stages of healing increases due to flame-flame interaction. Figure 4b shows a wide range of possibilities for premixed or nonpremixed edge flames in the reignition process. Extensive observation of the animations suggests that the combustion mode alters from nonpremixed at the beginning of the healing to premixed as the healing is advanced.

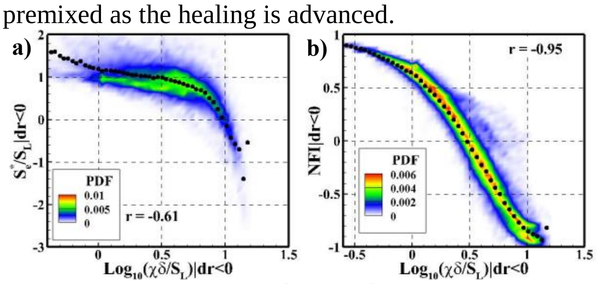

Figure 4. The joint PDF of a) edge-flame propagation velocity and b) NFI with the normalised scalar dissipation rate when holes are healing (black circles are conditional means).

5. Discussion

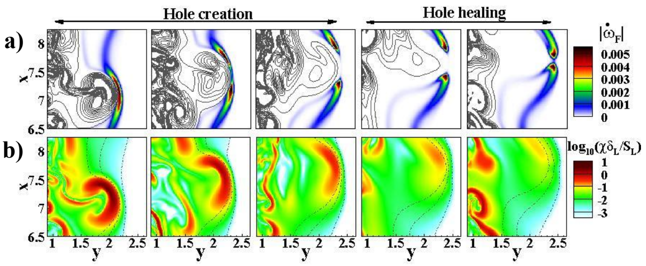

Figure 5. Instantaneous contour plots of a) reaction rate and b) scalar dissipation rates at local extinction and reignition (grey lines in a) are vorticity and dot-lines in b) are mixture fraction iso-contours).

To summarise the main findings, the instantaneous local extinction and reignition process for a given hole is presented in Fig. 5. As can be seen, the extinction occurs as a large structure hits the mixture-fraction iso-surface. After extinction, the scalar dissipation rate is high and the flame front has a comet shape similar to highly strained counter-flow flames [25]. The reignition process starts with propagation of the comet shape structures towards each other as the large structure moves away. It appears that the reignition starts with a nonpremixed structure, approaching a triple flame structure as the healing is progressed.

6. Conclusion

The local extinction and reignition in a turbulent lifted flame were studied using direct numerical simulation (DNS). The conditional mean of edge-flame propagation velocity on the scalar dissipation rate shows a good agreement with the predictions of the model proposed by Pantano and Pullin [6]. Separate analyses of extinction and reignition were performed. It was revealed that a high scalar dissipation rate is required for the extinction, whereas the generated hole can nonetheless grow with significantly lower values of scalar dissipation rate. The flame shows a nonpremixed nature during extinction while it can be either premixed or non-premixed during reignition.

7. Acknowledgments

This work was supported by the Australian Research Council (ARC). The research was also supported by access to computational resources on the Australian NCI National Facility through the National Computational Merit Allocation Scheme and Intersect Australia partner share.

8. References

[1] V. Favier, L. Vervisch, Combust. Flame **125** (1–2) (2001), pp. 788-803.

[2] V. Favier, L. Vervisch, Symp. (Int.) Combust. **27** (1) (1998), pp. 1239-1245.

[3] F. N. Egolfopoulos, Int. J. Energy Res. **24** (11) (2000), pp. 989-1010.

[4] C. Pantano, J. Fluid Mech. **514** (2004), pp. 231-270.

[5] P. Sripakagorn, S. Mitarai, G. Kosály, H. Pitsch, J. Fluid Mech. **518** (2004), pp. 231-259.

[6] C. Pantano, D. I. Pullin, J. Fluid Mech. **480** (2003), pp. 311-332.

[7] J. Hult, U. Meier, W. Meier, A. Harvey, C. F. Kaminski, Proc. Combust. Inst. **30** (1) (2005), pp. 701-709.

[8] K. M. Lyons, K. A. Watson, C. D. Carter, J. M. Donbar, Combust. Flame **142** (3) (2005), pp. 308-313.

[9] R. L. Gordon, A. R. Masri, E. Mastorakos, Combust. Flame **155** (1-2) (2008), pp. 181-195.

[10] S. Karami, E. R. Hawkes, M. Talei, J. H. Chen, J. Fluid Mech. **777** (2015), pp. 633-689.

[11] J. Göttgens, F. Mauss, N. Peters, Symp. (Int.) Combust. **24** (1) (1992), pp. 129-135.

[12] D. Garrido-López, S. Sarkar, Proc. Combust. Inst. **30** (1) (2005), pp. 621-628.

[13] A. Cessou, C. Maurey, D. Stepowski, Combust. Flame **137** (4) (2004), pp. 458-477.

[14] J. H. Chen, A. Choudhary, B. De Supinski, M. Devries, E. R. Hawkes, S. Klasky, W. K. Liao, K. L. Ma, J. Mellor-Crummey, N. Podhorszki, R. Sankaran, S. Shende, C. S. Yoo, Comput. Sci. Disc. **2** (1) (2009), pp.

[15] J. C. Sutherland, C. A. Kennedy, J. Comput. Phys. **191** (2) (2003), pp. 502-524.

[16] C. S. Yoo, Y. Wang, A. Trouvé, H. G. Im, Combust. Theor. Model. **9** (4) (2005), pp. 617 - 646.

[17] C. S. Yoo, H. G. Im, Combust. Theor. Model. **11** (2) (2007), pp. 259 - 286.

[18] E. R. Hawkes, R. Sankaran, J. H. Chen, Proc. Combust. Inst. **33** (1) (2011), pp. 1447-1454.

[19] E. Hawkes, R. Sankaran, J. Chen, 16th Australasian Fluid Mechanics Conference (AFMC) (2007), pp. 1271-1274.

[20] I. G. Boxx, C. D. Carter, W. Meier, AIAA SciTech, 13-17 January 2014, National Harbor, Maryland (52nd Aerospace Sciences Meeting) (2014), pp.

[21] R. Gordon, I. Boxx, C. Carter, A. Dreizler, W. Meier, Flow Turbul. Combust. **88** (4) (2012), pp. 503-527.

[22] S. Noda, H. Mori, Y. Hongo, M. Nishioka, JSME Int. J. B **48** (1) (2005), pp. 75-82.

[23] E. Knudsen, H. Pitsch, Combust. Flame **159** (1) (2012), pp. 242-264.

[24] N. Darabiha, Combust. Sci. Technol. **86** (1-6) (1992), pp. 163-181.

[25] G. Amantini, J. H. Frank, A. Gomez, Proc. Combust. Inst. **30** (1) (2005), pp. 313-321.